Analysis of the Principle and State-of-art Facilities of Mobile Atom Interferometry Gravity

Jinglei Chen*

University of Shanghai for Science and Technology, Shanghai, China

*Corresponding author: 2012140109@st.usst.edu.cn

Abstract. With over 20 years of development, atomic interferometry gravimeters have distinguished themselves in gravity measurements by their high precision and sensitivity. To cater to the demands of field absolute gravity measurements for marine and aerial gravity field measurements, resource exploration, inertial navigation, and positioning, the miniaturization, mobility, and engineering of atomic interferometry gravimeters have become crucial areas of development. On this basis, this article elucidates the principles of atomic interferometry gravimeters, encompassing various laser cooling techniques, magneto-optical traps, and Raman light interference. As a matter of fact, it provides an overview of the principles and achieved precision benchmarks of portable, vehicular, airborne, and shipborne atomic interferometry gravimeters. Additionally, it analyzes the experimental content and results of maritime, terrestrial, and aerial experiments based on portable atomic interferometry gravimeters. The limitations of portable atomic interferometry gravimeters are discussed, along with an exploration of their application prospects. Overall, these results shed light on guiding further exploration of mobile atom interferometry gravity.

Keywords: Laser cooling; Atom interferometry gravimeter; Absolute gravity measurement; Portable.

1. Introduction

Laser cooling has been developed for at least 30 years and serves as a cooling technique capable of cooling atoms or molecules to microkelvin levels. For Doppler cooling, moving atoms or molecules are irradiated by two beams of laser light with the same frequency but opposite propagation directions [1]. The frequency of the laser light is slightly lower than the frequency required for the atoms to transition to the excited state [1]. Due to the Doppler shift, the irradiated atoms have a higher probability of absorbing photons with opposite momentum, resulting in damping forces. The source of these damping forces is the momentum carried by photons [1]. For Sisyphus cooling, atoms are irradiated by two beams of laser light with the same frequency, opposite propagation directions, and opposite polarization directions. The kinetic energy of the atoms is converted into potential energy, which is later lost due to the emission of light, leading to the attenuation of the atoms' kinetic energy [2]. This process is similar to the Greek myth of Sisyphus pushing a stone, where the stone rolls down, and the process repeat.

Building upon laser cooling, people use magneto-optical traps and evaporative cooling to achieve Bose-Einstein condensation [3]. In practical applications, laser cooling is utilized to create atomic fountains for atomic clocks or atomic interferometry gravimeter. Analysis of atomic interferometry gravimeters has been ongoing for 20 years. With the advancement of technology, more advanced atomic interferometry gravimeters have been developed based on precision optimization and integration. This article focuses on portable atomic interferometry gravimeters, introducing their definitions and components. It then explains the principles of atomic interferometry and provides an overview of existing portable atomic interferometry gravimeters, their applications, and gravity measurements. Finally, limitations are summarized, and prospects are discussed.

2. Basic Descriptions of Mobile Atom Interferometry Gravity

Because the traditional atomic interferometry gravimeter is excessively bulky or its mass is too large, it is difficult to use for measuring gravity at different locations. This also results in limitations

in the practical application of traditional atomic interferometry gravimeters [4-7]. On the other hand, portable atomic interferometry gravimeters have undergone substantial integration in various systems, enabling them to be transported by different carriers. These carriers can be categorized as: manually portable, vehicular, elevator-compatible, shipboard, and airborne [8-11].

The portable atomic interferometry gravimeter consists of an electronic control system, an optical system, a vibration isolation system, and a carrier. In order to reduce the size and mass of the atomic interferometry gravimeter, integration has been implemented across various components, including the vacuum system, optical path system, circuit system, and laser system.

3. Principle

3.1. Laser Cooling

At room temperature, atoms exhibit significant thermal motion, resulting in high velocities. However, the vacuum tube size in which the atomic interference gravimeter operates is limited. On one hand, one requires atoms at low temperatures since at low temperatures, atoms exhibit wave-like properties, allowing control of their velocities to satisfy the resonance conditions with Raman light [12]. On the other hand, one aims for enhanced atom controllability. The technique of laser cooling enables deliberate control over atomic motion velocity and direction. When atoms are irradiated by laser light of a specific frequency, they can undergo stimulated absorption, transitioning to an excited state. Since photons possess momentum, based on the momentum principle, it can be assumed that the atom experiences a force directed to the right, as depicted in Fig. 1a). Here, the laser frequency ν is obtained from $E = h\nu$, where E represents the energy required for the atom to transition from the ground state to the excited state, and h is the Planck constant. The traditional form of laser cooling, namely Doppler cooling, is derived from this fundamental principle. When an atom with an initial velocity v is moving to the right (shown in Fig. 1b) and is illuminated by two laser beams of frequency ν_2 (where $\nu_2 < \nu$), the Doppler shift causes the frequency ν_2' of the left-propagating laser beam to increase, approaching ν, while the frequency ν_2 of the right-propagating laser beam decreases. This scenario increases the probability of the atom absorbing photons from the left-propagating laser beam, resulting in a force $\vec{F}$ directed to the left. Due to the opposing damping force in the direction of motion, the atom's velocity decreases, reducing the Doppler shift. Consequently, the damping force $\vec{F}$ decreases, leading to the cooling of the atom [1]. However, Doppler cooling has its limits, typically reaching temperatures in the range of a few hundred μk, which is related to the natural linewidth of the atom's excited state, as described by Eq. (1):

$$T_{doppler} = \frac{h\Gamma}{2k_B} \tag{1}$$

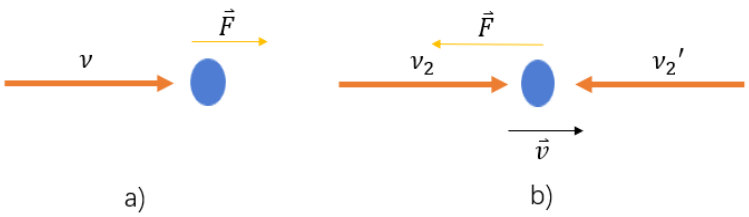

Fig. 1 Doppler Cooling

However, the limits of Doppler cooling cannot achieve the low temperatures required for resonance. Therefore, there is a need to explore a method that can cool atoms to even lower temperatures, and thus, one employs Sisyphus cooling [2]. In contrast to Doppler cooling, the laser polarizations used in Sisyphus cooling are mutually orthogonal. Typically, polarization states like $\sigma^+ - \sigma^-$ are used as shown in Fig. 2. Assuming the atoms are moving in the positive direction along the z-axis, the perturbing potential $V_{rot} = kvJ_z$ caused by the rotation of polarization states leads to changes in population distribution. Consequently, moving atoms have a 6-fold higher probability of

absorbing photons from σ^+ laser. Sisyphus cooling can typically achieve temperatures on the order of $10^{-1}\mu k$ [2]. When the atomic recoil kinetic energy from spontaneously emitted photons balances with the absorbed photon energy, the atom reaches the temperature limit of cooling. Refer to Eq. 2 for specifics, where k_B represents the Boltzmann constant:

$$T_r \approx \frac{\hbar^2 k^2}{m k_B} = \frac{h^2}{m k_B \lambda} \tag{2}$$

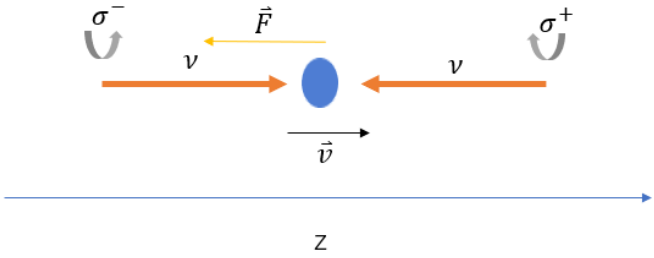

Fig. 2 Sisyphus cooling.

3.2. Magneto-optical Trap and Atom Fountain

Because the aforementioned one-dimensional cooling methods are not sufficient to confine atoms completely in three dimensions, a magneto-optical trap (MOT) is employed in the atomic interferometry gravimeter to trap the atoms. The magneto-optical trap is composed of a pair of counter-propagating Helmholtz coils and three pairs of circularly polarized laser beams with opposite propagation directions and opposite polarization directions [13]. The counter-propagating Helmholtz coils generate a linearly varying magnetic field as shown in Fig. 3a). This magnetic field, undergoing linear changes, induces a linear variation in the energy of atoms with quantum numbers $J = 1, M_J = 0, \pm 1$ due to the Zeeman effect $\Delta E \propto B \cdot M_J$. According to selection rules, atoms with $J = 1, M_J = 1$ can only be excited by σ^+ polarized laser light, while atoms with $J = 1, M_J = 0, \pm 1$ can only be excited by σ^- polarized laser light (as depicted in Fig. 4). The process of photon absorption results in a force acting on the atom:

$$F_{mot} = F_{\sigma^+}[\omega - kv - (\omega_0 + \beta y)] - F_{\sigma^-}[\omega + kv - (\omega_0 - \beta y)] \approx -2\frac{\partial F}{\partial \omega} \cdot kv + 2\frac{\partial F}{\partial \omega_0} \cdot \beta y \tag{3}$$

Additionally, since $\frac{\partial F}{\partial \omega} = \frac{\partial F}{\partial \omega_0}$, it follows that:

$$F_{mot} = -2\frac{\partial y}{\partial x}(kv + \beta y) = -\alpha v - \frac{\alpha\beta}{k} y, \alpha = 2\frac{\partial F}{\partial \omega} k \tag{4}$$

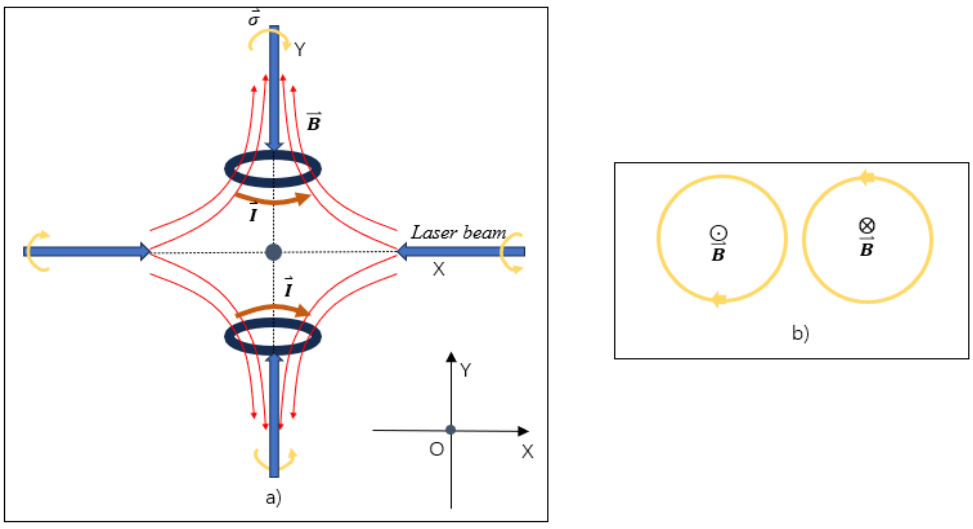

Fig. 3 Structure of magneto-optical trap.

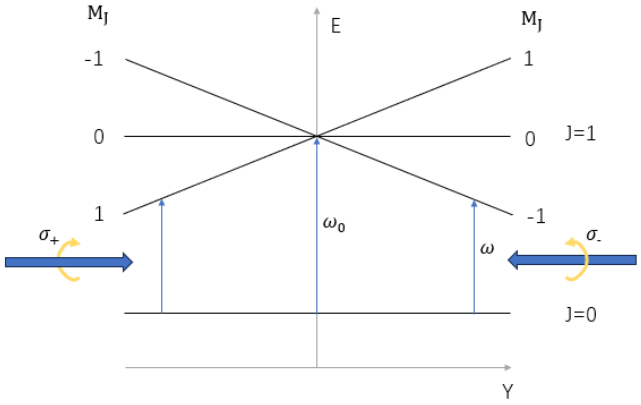

Fig. 4 Transition energy levels of atoms in magneto optical traps.

It's not difficult to see that when the atom is positioned at y > 0 (y < 0), it experiences a force directed towards the origin, and the magnitude of the force depends on its position. The atom behaves like a spring oscillator and eventually comes to rest at the origin. The same principle applies to the X and Z axes. The atomic fountain is based on the magneto-optical trap, and by increasing one of the laser frequencies in each set, the atom will experience a force along the body diagonal. This results in a projectile-like motion, influenced solely by gravity throughout the process – rising first and then falling back down [6].

3.3. Raman Light Interference

Raman light typically consists of a pair of counter-propagating laser beams with frequencies that are far detuned from the excited state. This far detuning aims to minimize spontaneous emission from the excited state (shown in Fig. 5a**)**, one laser beam has a wavevector $\overrightarrow{k_1}$, while the other laser beam has a wavevector $\overrightarrow{k_2}$. The effective wavevector is then defined as $\overrightarrow{k_{eff}} = \overrightarrow{k_1} - \overrightarrow{k_2}$. When the frequency difference between the two hyperfine levels of the atomic ground state matches the frequency difference between the two laser beams, an interaction occurs. As depicted in Fig. 5b, applying $\frac{\pi}{2} - \pi - \frac{\pi}{2}$ pulses results in a superposition of two atomic states. This leads to internal state interference, and the interference phase difference $\Delta\varphi = \varphi_1 - 2\varphi_2 + \varphi_3$ contains gravity-related information, expressed in the following formula:

$$\Delta\varphi = (\overrightarrow{k_{eff}} \cdot \vec{g} - 2\pi\alpha)T^2 \tag{5}$$

Where α represents the chirp rate of the Raman laser, $\vec{g}$is the acceleration due to gravity, and T is the interval between the two Raman laser pulses. From equation (3-3), it can be seen that when $\overrightarrow{k_{eff}} \cdot \vec{g} - 2\pi\alpha = 0$, regardless of how T changes, all interference fringes will intersect at a single point. By measuring the α value at this point, the value of the gravitational acceleration g can be obtained as $g = \frac{2\pi\alpha}{k_{eff}}$.

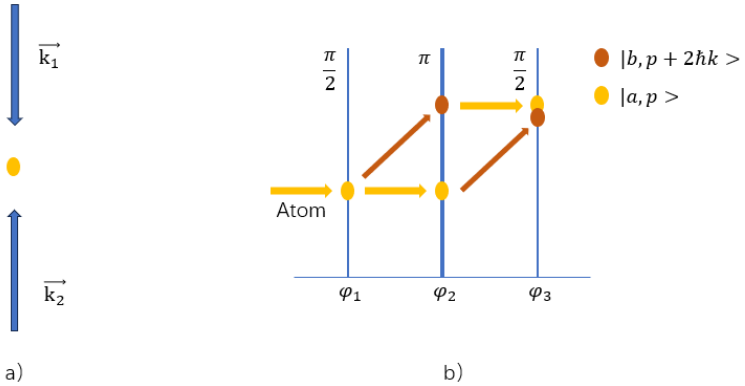

Fig. 5 Interaction between Raman light and atoms.

4. Facilities

Currently, atomic interferometry gravimeters can be roughly categorized based on their platforms as follows: shipborne atomic interferometry gravimeters, portable atomic interferometry gravimeters, vehicular atomic interferometry gravimeters, and airborne atomic interferometry gravimeters [8-11].

4.1. Shipborne Atomic Interferometry Gravimeter

In 2018, the Bidel group from France developed a shipborne atomic interferometry gravimeter (as shown in Fig. 6) [10]. Due to the relatively small variations in gravitational acceleration compared to the motion of the carrier, the values obtained from atomic sensors are inaccurate. Additionally, there are measurement dead zones during the preparation and detection of atomic samples, during which gravity is not measured. To overcome these two challenges, the Bidel group integrated the atomic sensor with a classical accelerometer. On one hand, the classical accelerometer can measure gravity conventionally to compensate for the unmeasured gravity due to dead zones. On the other hand, the classical accelerometer measures rough acceleration values to eliminate uncertainty and determine the signal of the atomic sensor. This atomic accelerometer is installed in a compact housing consisting of a cylinder with a diameter of 22 centimeters and a height of 52 centimeters. It includes a vacuum chamber made of glass, magnetic coils, optical components for generating all laser beams and collecting atomic fluorescence, two layers of metal shielding external magnetic fields, and a classical accelerometer. The uncertainty of this shipborne atomic interferometry gravimeter is 0.06 mGal, and its theoretical sensitivity reaches 0.8 mGal$\sqrt{Hz}$. However, due to challenging maritime conditions, the achieved precision is lower than $10^{-5}m/s^2$. Nevertheless, its accuracy far surpasses that of traditional spring gravimeters.

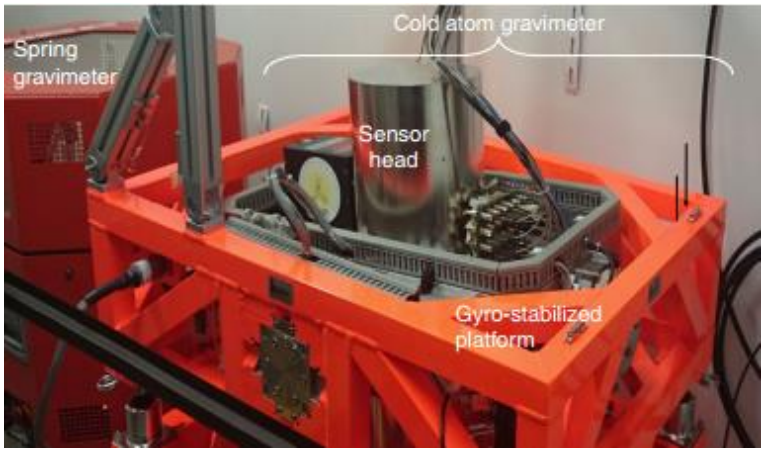

Fig. 6 Shipborne atomic interferometry gravimeter [10].

4.2. Portable Atomic Interferometry Gravimeter

In 2011, the Peter group from the University of Hamburg developed a portable atomic interferometry gravimeter called GAIN (as shown in Fig. 7). It was placed inside a small transportable truck. When measurements were required, the gravimeter would be taken out from the truck, enabling portable measurements. The gravimeter's sensitive head was housed within a transportable cage measuring 127cm × 82cm × 193cm and weighing 160kg. The traditional six-beam magneto-optical trap method was used for atomic confinement. The gravity measurement was conducted by vertically launching a cloud of atoms within a 750 mm long metal chamber, as depicted in Fig. 7b. The system was equipped with an actively isolated platform to reduce the impact of vibration noise. The apparatus achieved a sensitivity of 9.6 $\mu Gal/\sqrt{Hz}$, a stability of 0.05 μGal, and a precision of 3.9 μGal[14].

Fig. 7 Portable atomic interferometry gravimeter [14].

4.3. Vehicular Atomic Interferometry Gravimeter

In 2019, the Wu group developed a vehicular atomic interferometry gravimeter, the structure of which is depicted in Fig. 8. This gravimeter is characterized by its innovative pyramid-shaped magneto-optical trap (MOT). This structure holds several advantages. Firstly, it significantly accelerates the loading speed of atoms. Secondly, it reduces the impact of background atom refractivity, which is particularly crucial when the laser is slightly detuned. Lastly, due to the varying waist sizes, it offers a larger space for the magneto-optical trap and allows for higher-intensity Raman beams with limited laser power. The entire atomic interferometry gravimeter is mounted on a cart measuring $1m \times 0.8m \times 1.7m$, with a weight of 100kg. It utilizes a passive isolation platform to minimize the influence of vibration noise. The sensitivity of this system can reach 37 $\mu Gal/\sqrt{Hz}$, with an uncertainty of only 0.5 $\mu Gal/\sqrt{Hz}$ [9].

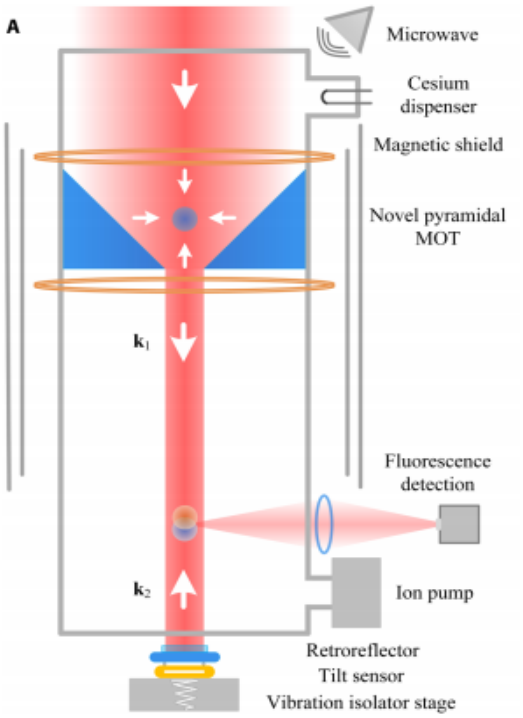

Fig. 8 Vehicular atomic interferometry gravimeter.

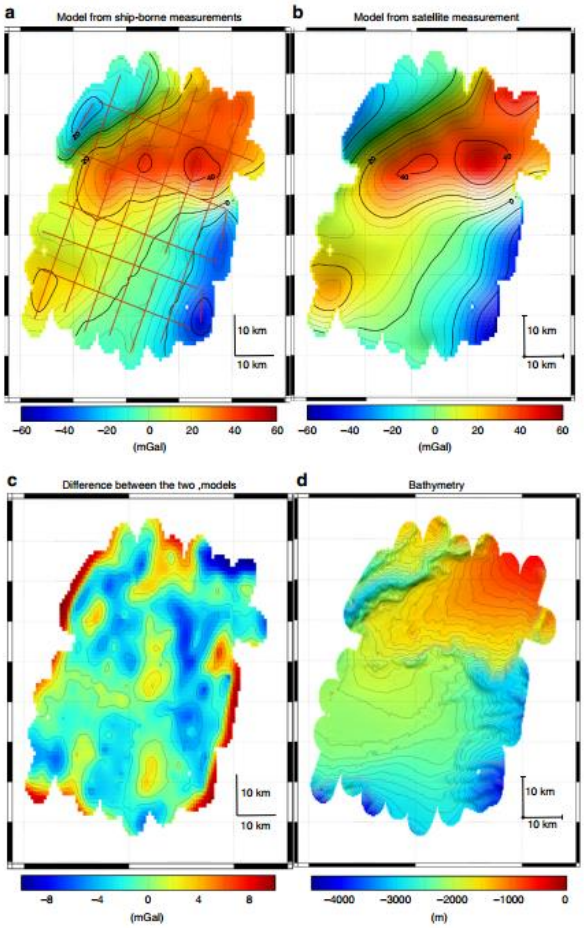

Fig. 9 Gravity anomaly model of Meriadzec terrace. A) Model obtained from ship-borne atom gravimeter measurements. The red lines are the profiles on which the gravity was measured. B) Model obtained from satellite measurements1 (Sandwell v24). C) Difference between the ship-borne model and the satellite model. The important differences on the left and right border are due to the extrapolation procedure of the ship-borne gravity measurements. D) Bathymetry for comparison with gravity anomaly.

4.4. Airborne Atomic Interferometry Gravimeter

In 2022, the Bidel group developed the GIRAFE airborne atomic interferometry gravimeter. Similar to the shipborne atomic interferometry gravimeter, the atomic sensor of GIRAFE is coupled with a conventional accelerometer to address the issue of acceleration uncertainty in measurements. Furthermore, this atomic interferometry gravimeter incorporates a hybrid algorithm. The algorithm operates when two signals exhibit good correlation within the range of $\frac{\lambda}{2T^2}$. The algorithm optimizes this correlation by adjusting T. As the correlation decreases, T is reduced, relaxing the need for closely matched correlations at the cost of sensitivity and precision loss [15]. The Bidel group compared the airborne measurement data with ground-based gravity data, finding a standard deviation range of 3.3 to 6.2 mGal and an average range of -0.7 to -1.9 mGal [11].

5. Application

5.1. Marine gravity measurement

The oceans cover 70% of the Earth's surface and constitute a vital component of the planet. Gaining a more detailed understanding of the structure of the oceanic gravity field contributes to accurate research on Earth's shape and internal composition. The Bidel group conducted grid measurements

of gravity along the Meriadzec plateau, an example of continental margin. They simulated the regional gravity model using GMT software and compared it with the satellite-derived gravity model. They found that the two models were similar, but the resolution of the model obtained from the atomic interferometry gravimeter was higher (as shown in Fig. 9) [10]. The mean difference between shipborne measurements and satellite models was 1.4 mGal, with a standard deviation of 2.4 mGal. This was consistent with the estimated error of shipborne measurements (0.9 mGal) and the estimated error of satellite models (2 mGal) [10].

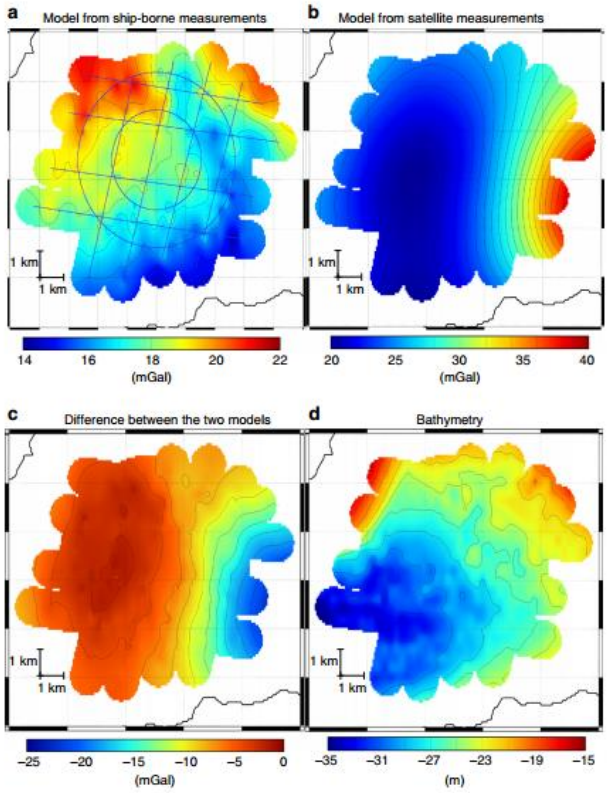

Fig. 10 Gravity anomaly model of Douarnenez bay. A) Model obtained from ship-borne atom gravimeter measurements. The blue lines are the profiles on which the gravity was measured. B) Model obtained from satellite measurements1 (Sandwell v24). C) Difference between the ship-borne model and the satellite model. D) Bathymetry for comparison with gravity anomaly.

Furthermore, the advantage of resolution was more evident in coastal regions. The Bidel group conducted gravity measurements in the Douarnenez Bay, performing measurements along eight straight lines at a speed of 8 knots for two rounds. The mean difference in gravity obtained was 0.1 mGal, with a standard deviation of 0.2 mGal. Subsequently, they measured gravity along circles with radii of 1.9 km and 3.3 km at speeds of 8 knots and 11 knots, respectively. The mean differences in gravity obtained were -0.2 mGal and 0.3 mGal, with standard deviations of 0.5 mGal and 0.6 mGal, respectively. The offset of gravity obtained from satellite models was 7.2 mGal, and the resolution was low (as shown in Fig. 10). This highlights the inaccuracy of satellite-derived gravity models in coastal regions and underscores the importance of the atomic interferometry gravimeter in these areas.

5.2. Ground gravity measurement

Resource and terrain exploration also require extensive gravity measurements. If done traditionally, this would demand significant human effort. However, the atomic interferometry gravimeter can effectively fulfill this task. By detecting subtle changes in gravity, one can obtain a rough topographical view of both the surface and subsurface (as shown in Fig. 11). The Wu group from the University of California, Berkeley, conducted gravity measurements at six locations in the Berkeley Hills, spanning 7.6 kilometers with an elevation change of nearly 400 meters (shown in Fig. 12). Using the measurement data, they calculated an average density of 2 g/cm^3 for the hills, which aligned

closely with data collected in 1998 [16]. Additionally, the team integrated their compact atomic gravimeter onto a truck and performed gravity measurements on flat roads and sloped roads [16].

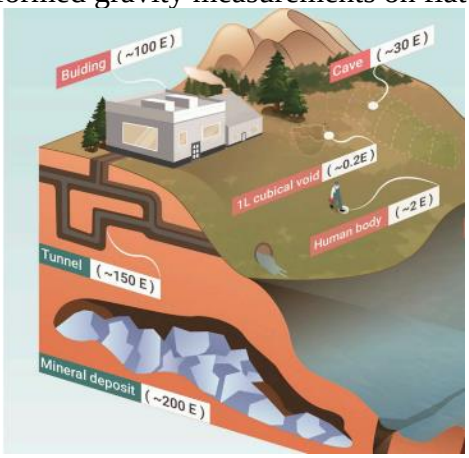

Fig. 11 Ground gravity measurement.

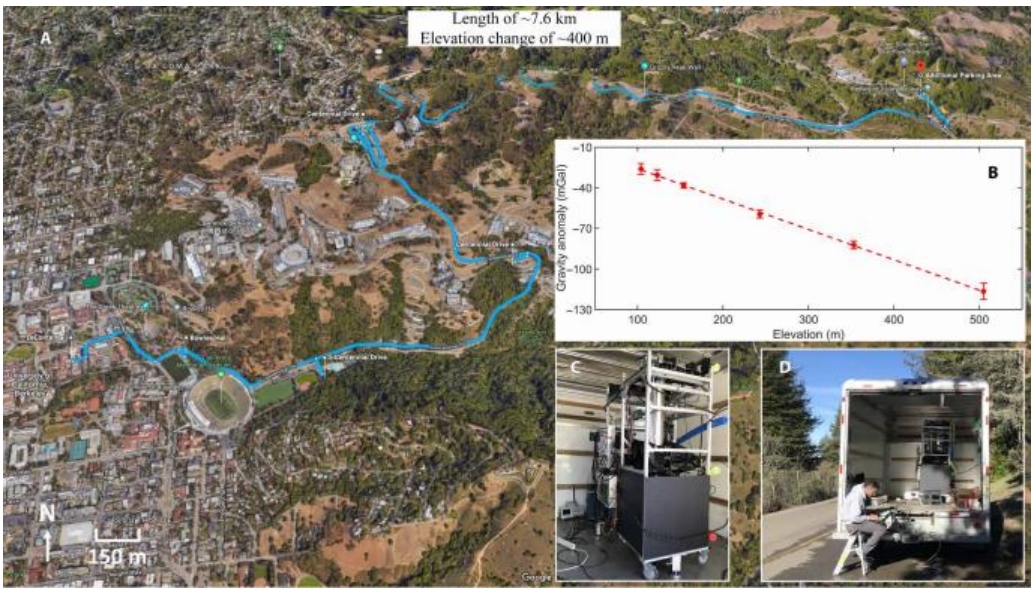

Fig. 12 Gravity measurement of Berkeley Hills.

5.3. Aerial Gravity Measurement

Aerial measurements offer great convenience due to the absence of terrain limitations and might become a common method for gravity measurements in the future. It could particularly simplify explorations across various terrains. The Bidel group conducted aerial gravity measurements in Iceland in 2020. Similar to the steps taken for the aforementioned maritime gravity measurements, they started by measuring gravity along straight lines between two locations and back. The results indicated that the repeatability of the gravimeter was within 3.9 mGal [15]. Subsequently, they compared their data with another set of ground-based gravity data. The standard deviation was less than 6.2 mGal, and the mean difference in gravity was less than -1.9 mGal [15].

6. Limitations and Future outlooks

It's evident that atomic interferometry gravimeters excel in gravity measurements and can accomplish measurements across different ranges or regions using various carriers. The obtained gravity models exhibit high precision, sensitivity, stability, and notable resolution compared to other gravity models. However, the portable atomic interferometry gravimeters presented in the article are still experimental instruments and have a certain way to go before commercialization. Additionally, these gravimeters heavily rely on isolation platforms, and severe vibrations could potentially affect

the final measurements. Furthermore, for areas with rugged terrain, measurements might be limited to airborne methods. Nevertheless, these challenges don't diminish the advantages of portable atomic interferometry gravimeters. It's highly likely that such instruments will eventually become a mainstream method for gravity measurements. Portable atomic interferometry gravimeters will find applications in fields such as vehicular and shipborne absolute gravity measurements, drone-based gravity measurements, and autonomous navigation for submarines.

7. Conclusion

This study analyses the principles and current status of portable atomic interferometry gravimeters. Firstly, the traditional laser cooling and its temperature limits are introduced. Subsequently, the core components of atomic interferometry gravimeters, namely the magneto-optical trap and the atomic fountain, are discussed. Secondly, the portable atomic interferometry gravimeters are categorized into four sections based on their carriers. The principles, dimensions, weight, precision, sensitivity, and stability of each category are presented. Next, the results of their gravity measurements are described, along with comparisons to satellite gravity models. It's observed that portable atomic interferometry gravimeters possess a high-resolution advantage while maintaining precision and sensitivity, relative to satellite gravity models. Despite susceptibility to measurement errors caused by carrier vibrations and unsuitability for certain terrains, these instruments place high demands on vibration isolation modules. Nevertheless, the merits of portable atomic interferometry gravimeters remain significant, and they are poised to become a mainstream method for gravity measurements. This article provides a clear explanation of atomic cooling techniques, magneto-optical traps, and atomic fountains. It enumerates advanced portable atomic interferometry gravimeters and summarizes their practical measurement applications. Furthermore, the potential applications and limitations are outlined, aiding readers in swiftly grasping the concept of portable atomic interferometry gravimeters.

References

[1] Wineland D J, Itano W M. Laser cooling of atoms. Physical Review A, 1979, 20(4): 1521.

[2] Cohen-Tannoudji C N, Phillips W D. New mechanisms for laser cooling. Physics Today, 1990, 43(10): 33-40.

[3] Bose-einstein condensation. Cambridge University Press, 1996.

[4] Marson I, Faller J E. g-the acceleration of gravity: its measurement and its importance. Journal of Physics E: Scientific Instruments, 1986, 19(1): 22.

[5] Kasevich M, Chu S. Measurement of the gravitational acceleration of an atom with a light-pulse atom interferometer. Applied Physics B, 1992, 54: 321-332.

[6] Dickerson S M, Hogan J M, Sugarbaker A, et al. Multiaxis inertial sensing with long-time point source atom interferometry. Physical Review Letters, 2013, 111(8): 083001.

[7] Křen P, Pálinkáš V, Vaľko M, et al. Improved measurement model for FG5/X gravimeters. Measurement, 2021, 171: 108739.

[8] Freier C, Hauth M, Schkolnik V, et al. Mobile quantum gravity sensor with unprecedented stability. Journal of physics: conference series. IOP Publishing, 2016, 723(1): 012050.

[9] Wu X, Weiner S, Pagel Z, et al. Mobile quantum gravimeter with a novel pyramidal magneto-optical trap. CLEO: QELS_Fundamental Science. Optica Publishing Group, 2020: JW2C. 5.

[10] Bidel Y, Zahzam N, Blanchard C, et al. Absolute marine gravimetry with matter-wave interferometry. Nature communications, 2018, 9(1): 627.

[11] Bidel Y, Zahzam N, Bresson A, et al. Airborne absolute gravimetry with a quantum sensor, comparison with classical technologies. Journal of Geophysical Research: Solid Earth, 2023: e2022JB025921.

[12] Davidson N, Lee H J, Kasevich M, et al. Raman cooling of atoms in two and three dimensions. Physical review letters, 1994, 72(20): 3158.

[13] Chu S, Hollberg L, Bjorkholm J E, et al. Three-dimensional viscous confinement and cooling of atoms by resonance radiation pressure. Physical review letters, 1985, 55(1): 48.

[14] Schmidt M, Senger A, Hauth M, et al. A mobile high-precision absolute gravimeter based on atom interferometry. Gyroscopy and Navigation, 2011, 2(3): 170-177.

[15] Bidel Y, Zahzam N, Bresson A, et al. Absolute airborne gravimetry with a cold atom sensor. Journal of Geodesy, 2020, 94: 1-9.

[16] Wu X, Pagel Z, Malek B S, et al. Gravity surveys using a mobile atom interferometer. Science advances, 2019, 5(9): eaax0800.

[17] Zhong J, Tang B, Chen X, et al. Quantum gravimetry going toward real applications. The Innovation, 2022, 3(3).